Military Technical College
Kobry El-Kobbah,
Cairo, Egypt.

15th International Conference
on Applied Mechanics and
Mechanical Engineering.

EFFECTS OF PROPELLER BLADE TWIST ON RECONNAISSANCE QUAD-ROTOR UAV

A. S. Imam* and R. Bicker**

ABSTRACT

Rotors play a pivotal role in the overall performance of a rotary-wing aircraft. Forces and moments required for flight are achieved through effective, compact and high-lift rotor design. Important rotor parameters are thrust, power and torque, which are functions of blade twist and rotor radius. A robust and efficient rotary-wing UAV flight control system must provide the vehicle with the ability to perform safe flight manoeuvres. This comprise normal flight conditions and proportionate regulation of thrust in response to the variation in power demand, which comes to play due to changes in aerodynamics conditions within the vehicle operating environment. This paper presents an in-depth analysis on the effect of variations of propeller blade twist and diameter with the view to designing an autonomous flight control system for a micro rotary-wing UAV. Virtual Blade Model (VBM) was used for the analysis and the result validated using a quad-rotor vehicle. The study comes up with an efficient propeller choice suitable for autonomous reconnaissance quad-rotor UAV.

KEY WORDS

Autonomous Flight Control System, Reconnaissance, RUAV, Rotors, Blade Twist, VBM and ANSYS FLUENT.

---

* PGR Student, Department of Mechanical and Systems Engineering, Newcastle University, U.K.

** Senior Lecturer, Department of Mechanical and Systems Engineering, Newcastle University, U. K.

INTRODUCTION

The development of unmanned aerial vehicles (UAVs) has increased during the last few years due its wide range of applications in both civil and military fields. In the military, UAVs can be used for applications such as kit delivery to troops in remote locations, extension of communication link in the combat zone, risk/damage evaluation, intelligence gathering and reconnaissance to mention but a few. The UAV's civil application includes search and rescue, disaster management, traffic control, border patrol, pipelines and power lines surveillance, etc. A new trend has evolved in recent times in the UAV's domain, where emphasis is now on the development of mini and micro rotary-wing aerial vehicles (RUAV). This is due to their unique capabilities of vertical take-off and landing. Hence, it requires no runway and has the advantage of being able to backpack and deploy by a soldier in all phases of operations. Reconnaissance is the military term used to refer to an operation which involves a force operating beyond its main forces to explore enemy's position and gain information about enemy forces or environment features. Designing a robust and effective RUAV flight controller for reconnaissance operation requires an in-depth study and understanding of the vehicle aerodynamics which is challenging because the aerodynamics flow field generated by a rotary-wing aircraft is extremely complicated and difficult to measure, model and predict. The rotor of a rotary-wing aircraft provides three functions: generation of thrust to overcome the vehicle weight and gravity, generation of horizontal propulsive force for forward flight and means of generating forces and moments for attitude and position of the vehicle in three-dimensional space to overcome disturbances.

A number of researchers have addressed the issue of aerodynamics of RUAVs operating in an outdoor environment at higher flight speed [1-3]. At high speeds, several aerodynamics effects significantly impact the flight characteristics and invariably the flight control system performance. These effects manifest as nonlinear disturbances on the rotor and airframe, thereby causing an increase or decrease in rotors' loading with attendant rise or fall in power demand as demonstrated in [4]. Effects of blade flapping and total thrust variation have been studied [5] and [6] where uncertainties, such as wind and saturation on RUAV blades, were considered.

AERODYNAMICS OF RUAV ROTORS

The lifting capability of any part of a rotating blade is related to its local angle of attack (AoA) and local dynamic pressure. The blade position is defined in terms of an azimuth angle, which is zero when the blade is pointing downstream. There are two basic flight conditions associated with a rotary-wing aircraft, namely: hover flight condition and forward flight condition.

Hover Flight

Hover is a special flight condition attainable only with a rotary-wing aircraft. In hover, the vehicle has zero forward speed and zero vertical speed: no climb, no descend. Therefore, the rotor flow field is azimuthally axisymmetric. By Momentum theory, the rotors thrust is related to the induced velocity and ideal power required to hover by:

$$V_i = \sqrt{\frac{T}{2\rho A}} \tag{1}$$

The ratio T/A is the disk loading, while TP is power loading and deal power required to hover is:

$$P = TV_i = T\sqrt{\frac{T}{2\rho A}} = \frac{T^{3/2}}{\sqrt{2\rho A}} \tag{2}$$

In hovering flight, Fig. 1, thrust equals weight and velocity variation along the blade is azimuthally axisymmetric and radically linear, with zero flow velocity at the rotational axis and the velocity reaching maximum *(V_{tip})* at the blade tip, Equation (3). The rotor thrust is proportional to the square of the tip velocity, Equation (4) and rotor power, *P,* depends on the cube of the tip speed, Equation (5).

$$V_{tip} = \Omega R \tag{3}$$

$$T \propto V_{tip}^2 \tag{4}$$

$$P \propto V_{tip}^3 \tag{5}$$

Forward Flight

However, in forward flight the rotors are required to produce both lifting and propulsive forces and must be tilted forward at prescribed AoA relative to the incoming flow. This results in blade being subjected to prescribe cyclic pitch angle and other cyclic flapping, lagging and dynamic deforming motion. The rotors encounter a maximum asymmetric velocity field at the blade that advances into the relative wind and minimum on the blade that retreats away from the relative wind. Furthermore, in forward flight, a component of the free stream, V_∞, adds to or subtracts from the rotational velocity at each part of the blade as shown in Fig. 2. Hence, V_{tip} becomes:

$$V_{tip} = \Omega R + V_\infty sin\psi \tag{6}$$

Under forward flight conditions, the rotors move through the air with an edgewise component of velocity that is parallel to the rotors' plane. Therefore, the mass flow rate, $\dot{m}$ through the rotors is given by:

$$\dot{m} = \rho AU \tag{7}$$

and the induced velocity and rotor total power are in Equation (8) and (9).

$$V_i = \frac{T}{2\rho AU} \tag{8}$$

$$P = TV_i = \frac{T^2}{2\rho AU} \tag{9}$$

where, U is the resultant relative velocity (disturbance).

PROBLEM FORMULATION

At higher forward flight speeds, the inherently asymmetric nature of the flow over the rotor disk gives rise to a number of aerodynamic problems, which eventually limits the rotor performance. The most obvious is that the blade tips on the advancing side of the rotor disk can start to penetrate into the super-critical and transonic flow regime, with the associated formation of compressibility zones and ultimately strong shock waves, hence result in much more power to drive the rotors. The increased power demands placed on the rotor systems coupled with the manifestation of compressibility effects, eventually limit forward speeds.

On the retreating side of the disk, the local velocity and dynamic pressure on the blade are relatively low and the blades operate at higher AoA to maintain lift. At higher AoA, stall ensued, which results in overall lost in lifting and propulsive capability and further deterioration in forward speed. The unsteady air-loads produced during dynamic stall are additional sources of vibration on the vehicle which can affect the effectiveness of various sensors on-board. A more accurate flight control system design must also account for aerodynamic interaction effects which exist between the rotor wakes and airframe. Therefore, appropriate selection of the propeller is paramount in ensuring robustness in the overall performance of the vehicle. Parameters of interest in the propeller design are blade twist (BT), chord, diameter and air-foil shape.

However, understanding the aerodynamics of micro rotary-wing UAVs involve the application of scaling rules to the analytical theories, seldom, these have many flaws. Numerical modeling remains about the best alternative means upon which the aerodynamics of micro rotary-wing aircrafts can be understood and then validated through experiment.

MODELING METHOD

Computational Fluid Dynamic (CFD) modelling method was used in this study. Utilizing Virtual Blade Model (VBM) under ANSYS FLUENT environment and the result was verified experimentally. The basic principle of the CFD modelling method is that the simulated flow region is divided into small cells within each of which the flow either kept under constant conditions or varied smoothly. Differential equations of momentum, energy, and mass balance are discretized and represented in terms of the variables at the centre of or at any predetermined position within the cells. These equations are solved iteratively until the solution reaches the desired accuracy [7].

ANSYS FLUENT

ANSYS FLUENT provides modelling capabilities for a wide range of incompressible and compressible fluid flow in either laminar or turbulent region. It combines a broad range of mathematical models for transport phenomena with the ability to model complex geometries. ANSYS FLUENT solves conservation equations for mass and momentum as well as equation for energy conservation if the flow involves heat transfer or compressibility. Additional transport equations are also solved when the flow is turbulent.

ANSYS Solution Method

Flows involving moving parts, such as turbines, fans, helicopter rotors are solved using the non-inertial reference frame. In these flow types, the interest is on the flow around the moving parts and their interaction. Therefore, equations of motion are altered to incorporate additional acceleration terms which occur due transformation from inertial reference to the moving reference frame. This allows the steady-state modelling of the problem with respect to the moving reference frame. There are numerous ANSYS models for flows involving moving parts, which include Sliding Mesh Model (SMM), Multiple Reference Frame (MRF), Mixing Plane Model (MPM), FAN Model and Virtual Blade Model (VBM) among others. However, since the objective of this study is to model the time average cumulative effects of the rotating blades, VBM will be used.

Virtual Blade Model

The VBM is an ANSYS Fluent model developed to fill a void in the rotating flow models; FAN, Sliding Reference Frame/Moving Reference Frame (SRF/MRF) for applications where the objective is to model the time-averaged cumulative effects of the rotating blades. Unlike FAN model, VBM takes into account the local effects due to blade twist, blade section aerodynamics, tapering, chord variation, local flow incidence angles, etc. Thus, the VBM is significantly more accurate than the FAN model and is indeed close to the SRF/MRF model without the punitively large cell count caused by the requirement to mesh the rotor blades with sufficiently fine resolution to obtain reasonably accurate flow fields.

VBM replaces the rotor systems with momentum sources on an actuator disk, allowing the pressure jump across the disk to vary with radius and azimuth. This eliminates the need to generate individual meshes over each of the rotor blades yielding computational meshes with substantially lower cell count while reducing significantly mesh generation time. The magnitude of the momentum sources is obtained from using the Blade Element Theory (BET), allowing for varying twist, chord and airfoil types along the span. The non-linear aerodynamic interaction between the rotor systems with each other and other structural components is solved by coupling the BET with the governing flow field equations as solved by ANSYS FLUENT.

THE FUNDAMENTAL GOVERNING EQUATIONS

Many of the aerodynamic problems found on the rotary-wing aircrafts involve viscous effects and the generation of turbulence. These effects are important in the 3-D turbulent boundary layers found on the blades and airframe, unsteady flow separation and dynamic stall, and in the rotor-airframe interaction. The Naiver-Stokes and Spalart-Allmarus equations are the fundamental equations governing the fluid dynamics of the rotary-wing aircraft. They encompass the principles of the conservation of mass; momentum and energy interchange within a fluid. In this application, only conservation of mass and momentum were considered, as it does not involve energy interchange. Equation (10) is Navier-Stokes mass conservation and momentum conservation equations while Equation (11) represents the three dimensional Navier-Stokes equations written in conservation form.

$$\frac{\partial \rho}{\partial t} + \nabla.(\rho \bar{v}) = S_m \quad (10)$$

$$\frac{\partial \rho}{\partial t} + \nabla.(\rho \bar{v} v) = -\nabla p + \nabla.(\bar{\bar{\tau}}) + p\bar{g} + \bar{F} \quad (11)$$

where p is the static pressure, $\bar{\bar{\tau}}$ is the stress tensor gravitational body force and external body force.

VEHICLE MODEL AND SOLUTION

The vehicle adopted was quad-rotor UAV designed and developed as part of this research at Robotics Laboratory, Newcastle University. Table 1 depicts the vehicle's characteristics. The simulation model was developed using ANSYS Design Modeller as shown in Fig 3.

The simulation aim was to study the effects of varying propeller blade twist with the view to selecting an optimum propeller combination and designing a robust and efficient autonomous flight control system for reconnaissance quad-rotor UAV. The study investigated the relationship between rotor speed, thrust and power for the vehicle in hover flight at 1m/s wind speed. The simulation was conducted with 250mm diameter propellers, having blade twist set at 15^0, 25^0 and 35^0. The study also focused on appreciation of the flow field interaction between the four rotors and the fuselage with the view to estimating how that interaction and aerodynamics disturbance (particularly, the wind) affects power demand and thrust generation. However, power, thrust and torque are related by:

$$C_T = \frac{T}{\rho \pi R^4 \Omega^2} \quad (12)$$

$$\tau = T C_T \quad (13)$$

$$P = \omega \tau \quad (14)$$

where C_T is the coefficient of thrust, T, the thrust (N), R, the blade radius and Ω, the angular speed in rpm, P, the power (Watts) and τ is the torque (Nm).

Simulation Setup

The model was meshed using ANSYS FLUENT mesher Fig. 4 and exported to FLUENT solver. The vehicle hover flight was simulated using the VBM and a user-defined-function source terms. The simulation settings were as follows:

i. **General**
- Solver type - Pressure based
- Velocity formulation - Absolute
- Time - Steady state

ii. **Models**
- Energy transport - Off
- Viscous - Strain/Vorticity-Based Spalart-Allmaras

iii. **Materials**
- Working Fluid - Air at standard atmospheric condition
- Free stream (wind speed) - 1m/s

iv. **Solution method**
- Couple scheme - Pressure-Velocity
- Spartial discretization - Green-Gauss-Node-Base gradient
- Pressure - PRESTO!
- Momentum - Second Order Upwind
- Modified turbulent viscosity - Second Order Upwind

VBM Setting

The VBM model, Fig. 5 was invoked and the general settings were filled with the rotors parameters as indicated in Table 2. The rotor-geometry-input, defines the rotor geometry in terms of airfoil type, shape, chord length and twist. These parameters were also filled as contained in Table 3.

RESULTS AND EXPERIMENT VALIDATION

The primary objective of this investigation was to establish the thrust and power variations due changes in rotor blade twist.

Simulation Results

The converged model indicates a nonlinear relationship between power and thrust, thrust increases with increase in power. The model also indicates higher power generation as the blade twist increased from 15^0 to 25^0 and 35^0 shown in Fig. 6, having the highest power at 35^0 blade twist. Conversely, blade twist at 25^0 produces greater thrust, Fig. 7. For instance, at 8000 rpm power and thrust distributions are: 6N and 200W @25^0 blade twist, while 5N and 320W @35^0 blade twist, Fig. 8. Similarly, rotors-fuselage flow field interaction shows significant turbulence as shown in the contour of velocity magnitude Fig. 9 and 10. This further confirms Equation 3, that maximum speed is at the blade tip. The high turbulence nature of the flow and strong structural interaction are potentially vibration and noise contributors to the system.

Experimental Setup and Results

An experimental validation rig was setup at Newcastle University's robotic laboratory as shown in Fig. 11. An embedded program was written in C language and ported to a dsPIC microcontroller. Components making up the system consist of BLDC motor drivers/drivers, inertial measurement unit (IMU) and ultrasonic sensor. The experiment was conducted with a propeller having blade twist @25^0, being the optimum as realized from simulation. The program runs an algorithm that spins the rotors to a defined hover height in 10 steps, each corresponding to a certain rotor speed. A provision of a minute delay was made to allow for measurement of the rotor speed and thrust. Experiment and simulation results strongly agree closely with largest thrust deviation of about 14% (0.3N) between 4000rpm and 7000rpm as shown in Fig 9.

CONCLUSION AND FUTURE WORK

In this paper, the effects of varying blade twist of a reconnaissance quad-rotor UAV have been studied with the view to choosing best propeller combination in order design an efficient and robust autonomous flight control system. Simulation results obtained from VBM in the ANSYS FLUENT environment and validated experimentally show close agreement. The results indicated that for a reconnaissance quad-rotor UAV having the configuration stated in this paper should have an optimum propeller blade twist @25^0 for effective performance. However, propeller optimality does not only depend on the blade twist but also on diameter, wind speed and direction. Therefore, future work will entail varying the propeller diameter, wind speed and direction to establish their effects on the overall system.

REFERENCES

[1] Wang, S. and Xiao-hui, Q., Aerodynamic Data Model Analysis and Simulation of Ducted Fan UAV, Electronics, Communications and Control (ICECC), 2011 International Conference on, vol., no., pp.699-702, 9-11 Sept. 2011.

[2] Rauf, A., Zafar, M.A., Ashraf, Z. and Akhtar, H., Aerodynamic Modelling and State-Space Model Extraction of a UAV using DATCOM and Simulink, Computer Research and Development (ICCRD), 2011 3rd International Conference on , vol.4, no., pp.88-92, 11-13 March 2011.

[3] Meng, I. Liu, L. and Veres, S.M., Aerodynamic Parameter Estimation of an Unmanned Aerial Vehicle Based on Extended Kalman Filter and its Higher Order Approach, Advanced Computer Control (ICACC), 2010 2nd International Conference on , vol.5, no., pp.526-531, 27-29 March 2010.

[4] Ilan, K. and Peter, K., Development of the Mesicopter: A Miniature Autonomous Rotorcrafts. In *American Helicopter Society Vertical Lift Aircraft Design Conference*, 2000.
[5] Gabriel H., Steven, W. and Claire, T., Starmac 2 Quadrotor Helicopters, IROS MAV Workshop, November 2007.
[6] Haomiao, H., Hoffmann, G. M., Waslander, S.L. and Tomlin, C.J., Aerodynamics and Control of Autonomous Quadrotor Helicopters in Aggressive Manoeuvring, IEEE International Conference on Robotics and Automation, 2009. ICRA '09, pages 3277–3282, May 2009.
[7] Allied Environment Technologies Inc., Computational Fluid Dynamics Modelling, Application for Engineering Solutions, (2007).

FIGURES AND TABLES

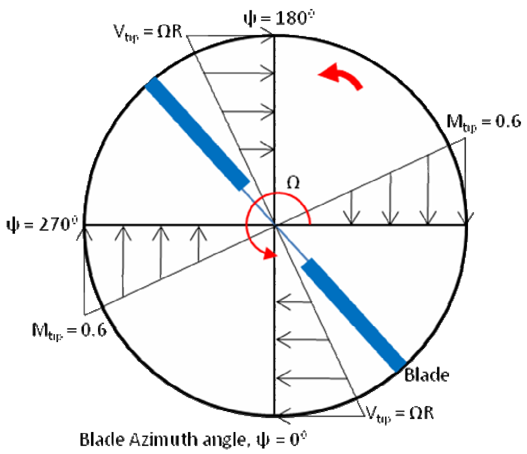

Fig. 1. Rotor in hover flight.

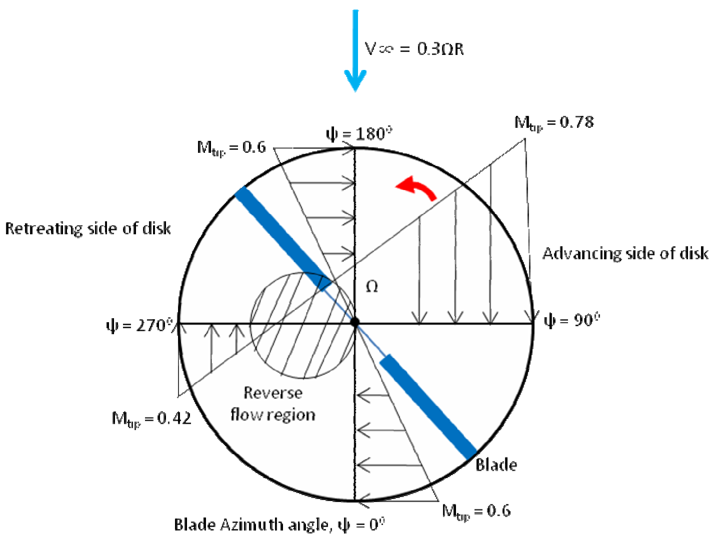

Fig. 2. Rotor in forward flight.

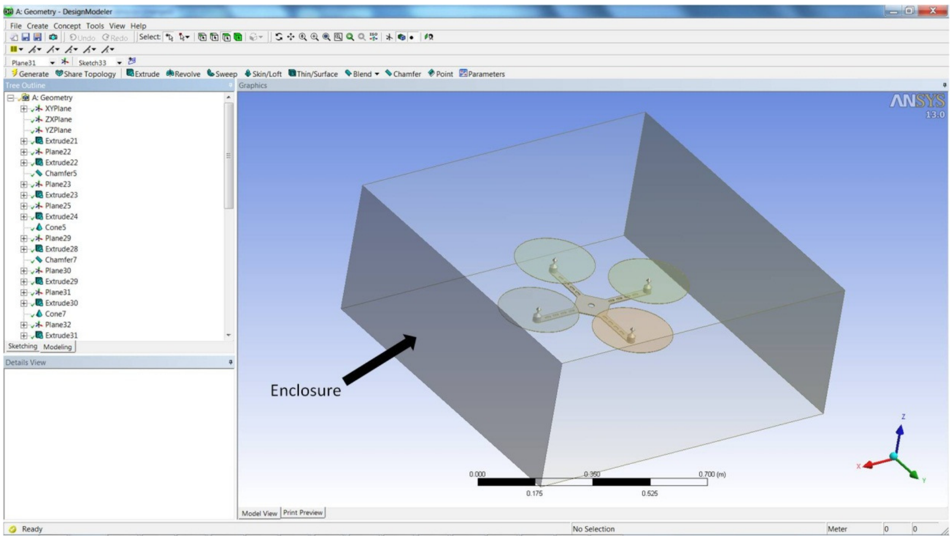

Fig. 3. Quad-rotor model.

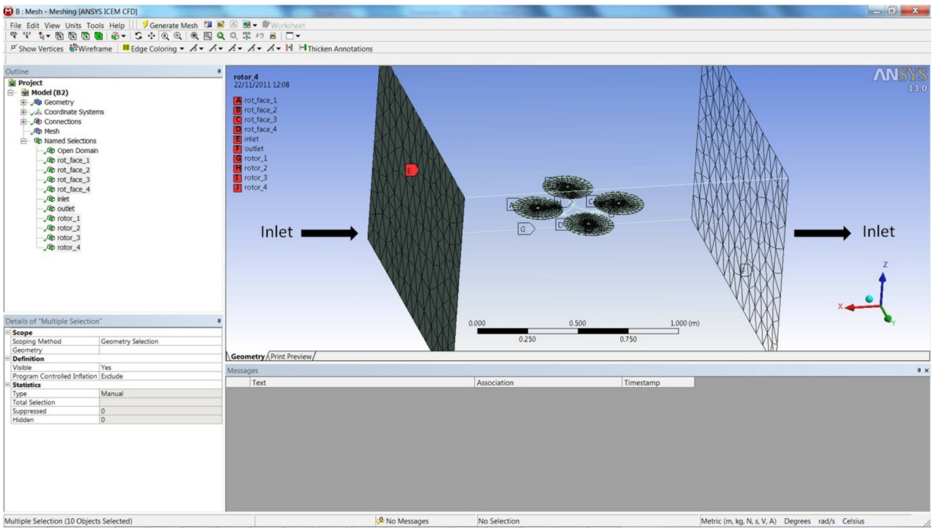

Fig. 4. Meshed quad-rotor model.

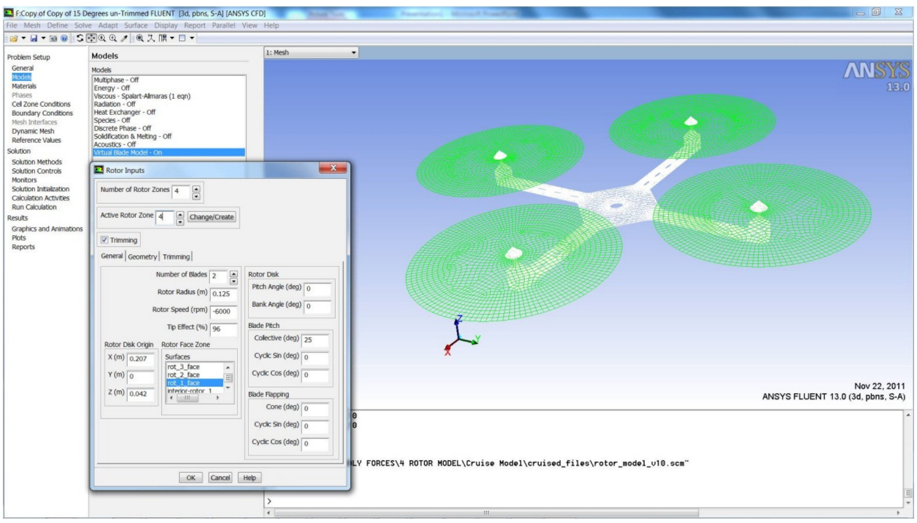

Fig. 5. VBM settings.

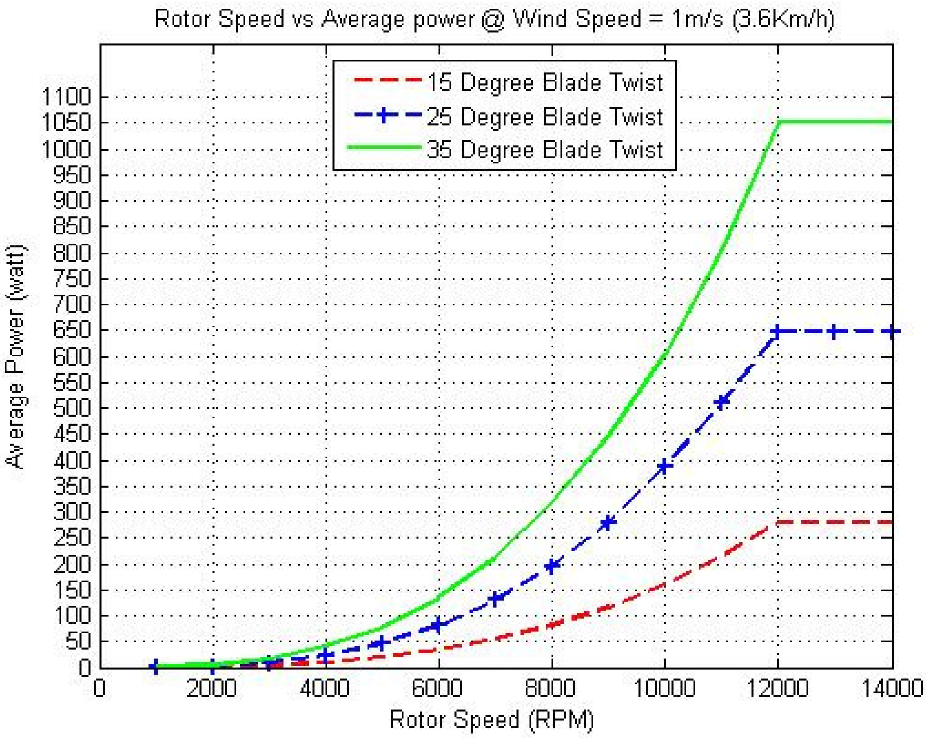

Fig. 6. Simulation results - rotor speed vs power.

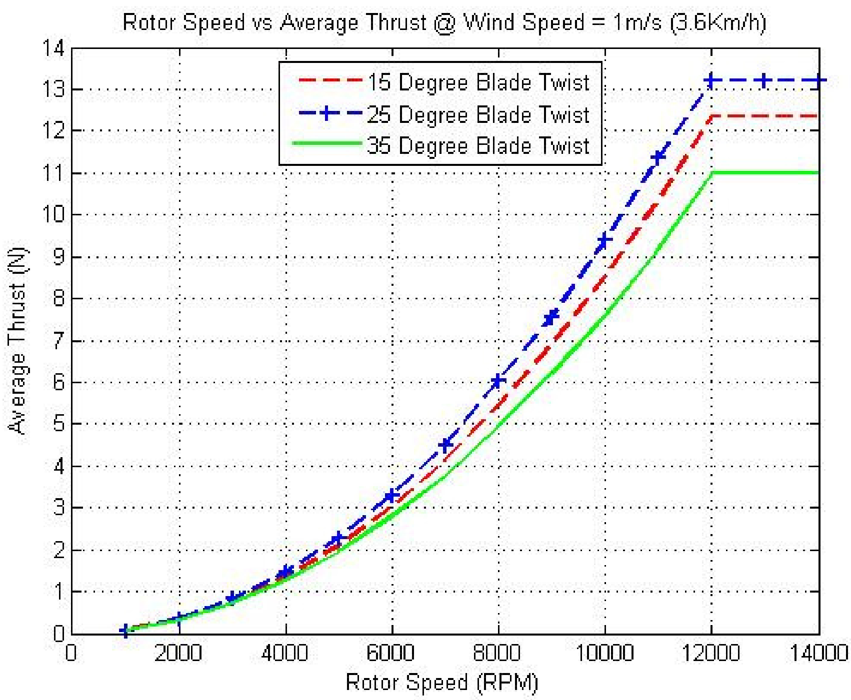

Fig. 7. Simulation results - rotor speed vs thrust.

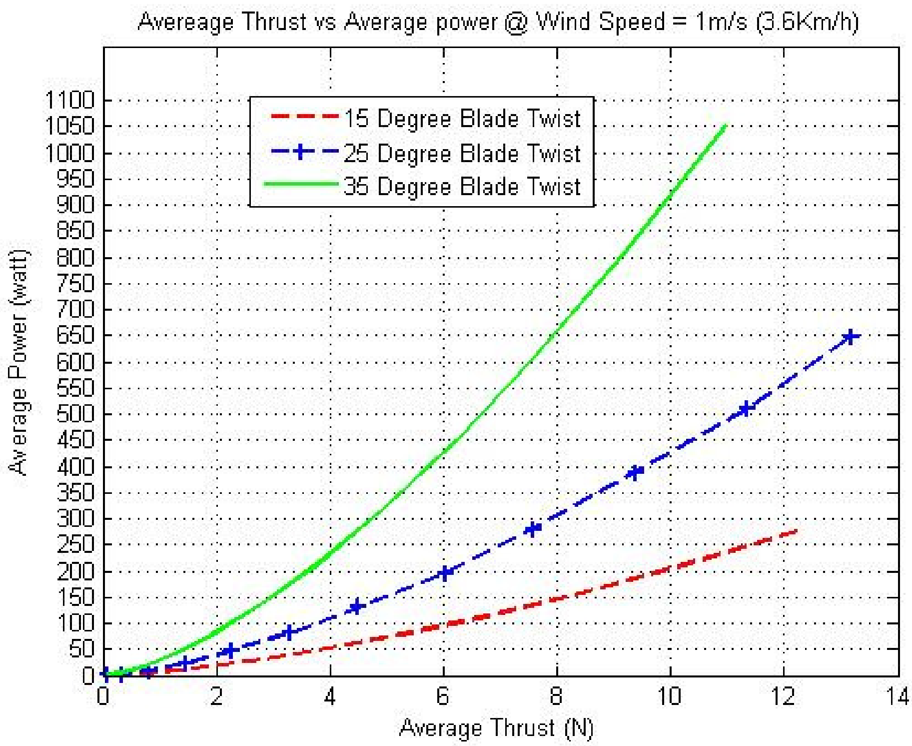

Fig. 8. Simulation results – thrust vs power.

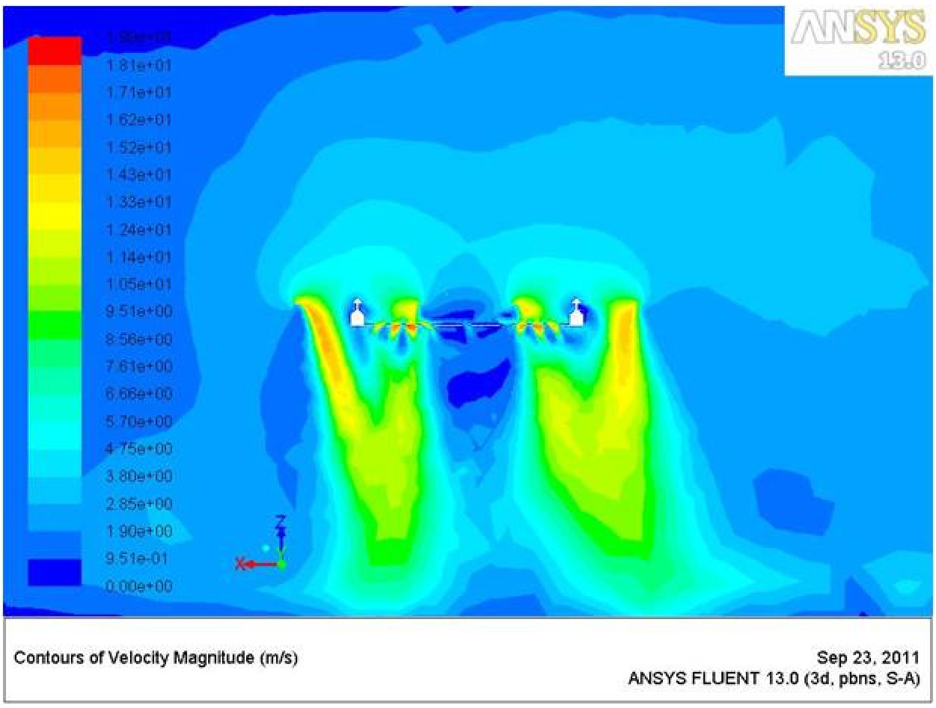

Fig. 9. Contours of velocity magnitude - rotors-fuselage flow field interaction – side

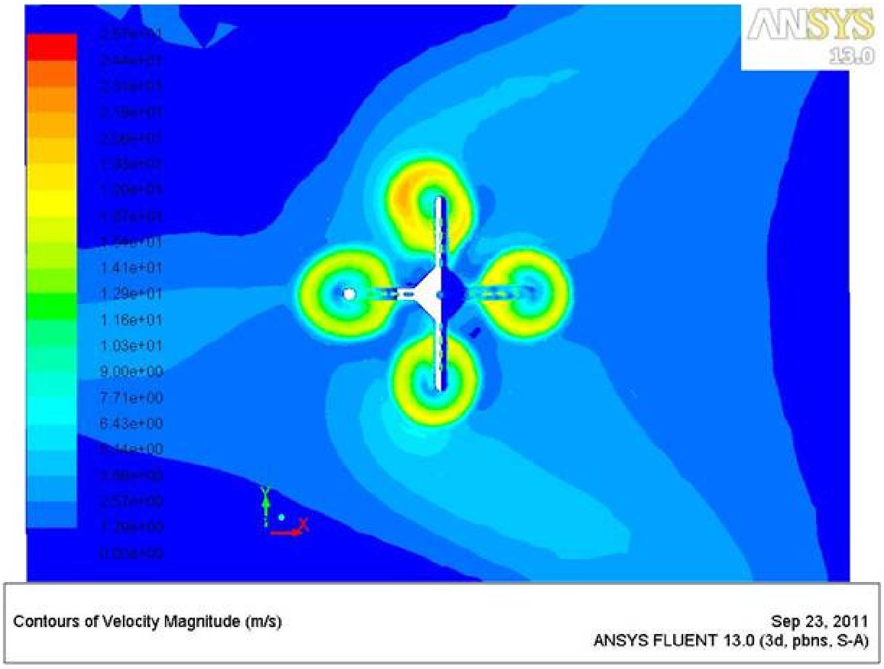

Fig. 10. Contours of velocity magnitude - rotors-fuselage flow field interaction – top.

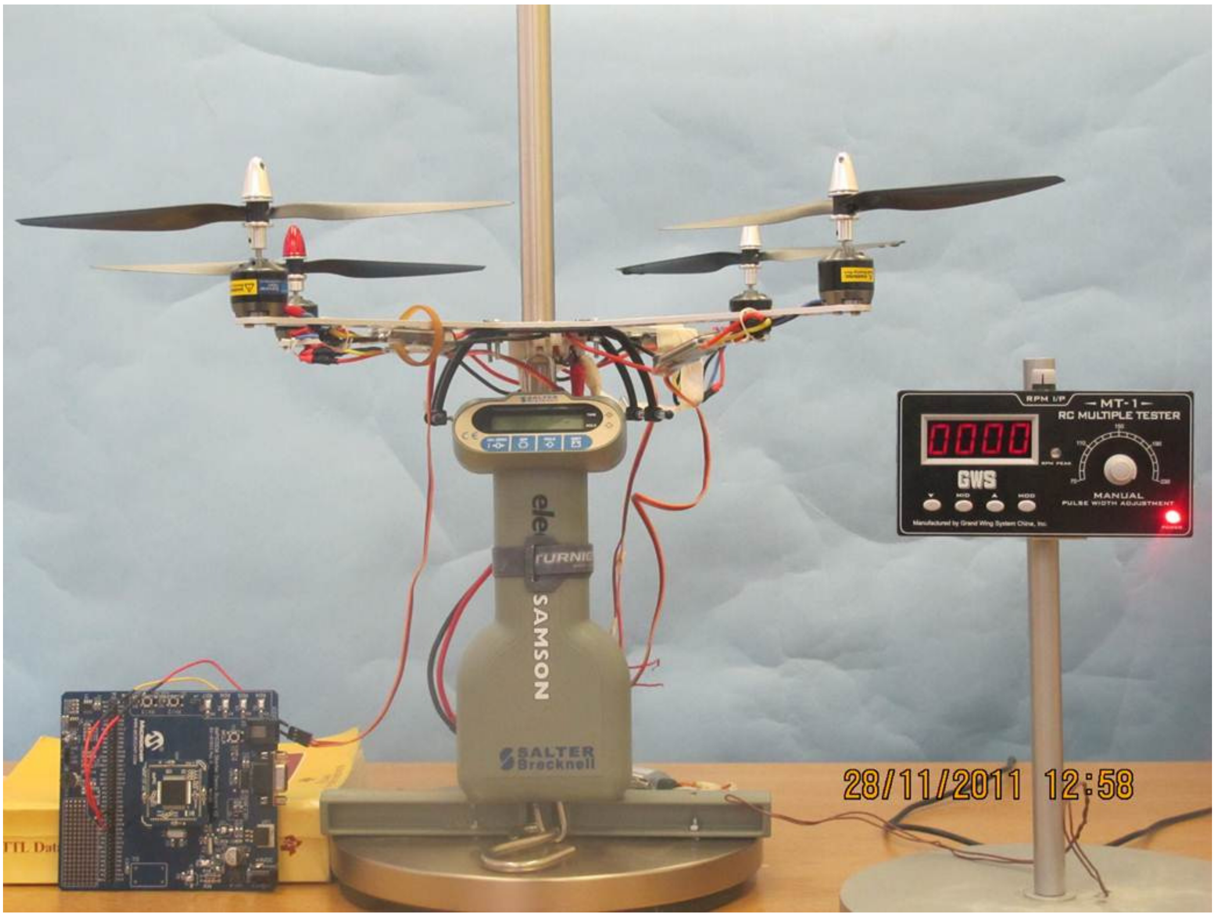

Fig. 11. Experiment rig.

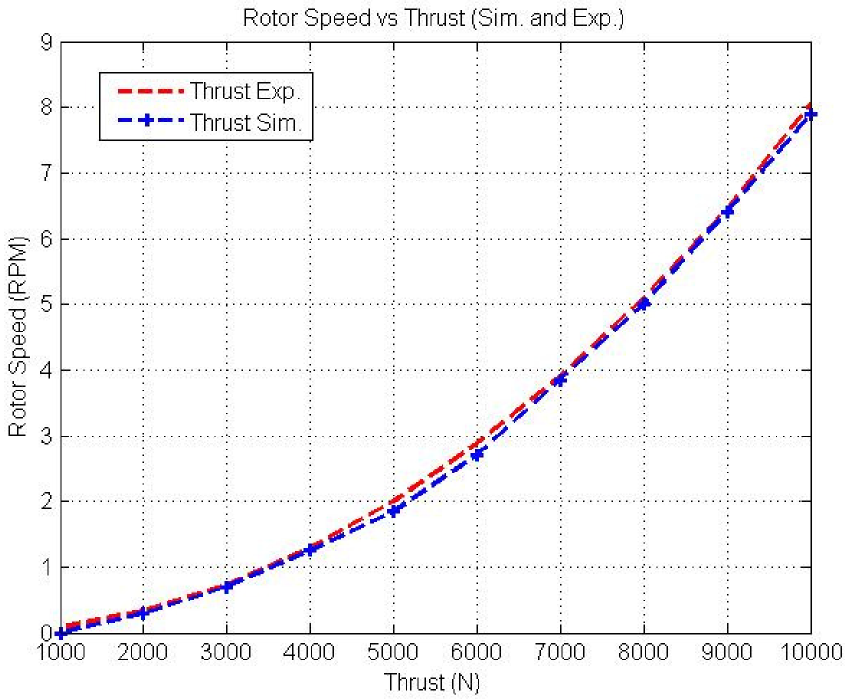

Fig. 12. Rotor speed vs experimental and simulated thrust.

Table 1. Quad-rotor vehicle characteristics.

Serial	Parameter	Value	Remarks
1	Material	3mm Aluminuim plate	
2	Vehicle weight	0.6 Kg	
3	Takeoff weight	1Kg	
4	Arm length	0.22 m	
5	Dimension	0.44 m	
6	Rotor raduis	0.125 m	

Table 2. VBM settings - rotor parameters.

Number of rotor zones	4
Active rotor zones	4
Rotor raduis	0.125 m
Tip effective	96%
Rotor disc origin	Rotor1 = (0.21, 0, 0.045) m
	Rotor2 = (0, -0.21, 0.045) m
	Rotor3 = (-0.21, 0, 0.045) m
	Rotor4 = (0, 0.21, 0.045) m
Rotors speed	1,000 - 10,000 rpm

Table 3. VBM settings – rotor geometry input

Serial	Raduis = (r/R)	Chord (m)	Twist	Airfoil Type
1	0	0.01	15 degress	naca0015
2	0.2	0.01	15 degress	naca0015
3	0.6	0.025	15 degress	naca0015
4	1	0.01	15 degress	naca0015